SOPHION BIOSCIENCE | Discover more

Application Report

Using Automated Patch Clamp for recordings of neuronal action potentials

Including a functional classification of hiPSC-derived neurological disease models based on single-cell firing patterns

Summary

Human-induced pluripotent stem cells (hiPSCs) are used for the generation of neuronal subtypes and neurological disease models. Electrophysiological measurements of ion-channel currents and action potentials are important functional indicators in these models. However, in practice, the intercellular variability in functional maturity within a population of hiPSC-derived neurons has made such studies challenging, especially in combination with the low-throughput nature of manual electrophysiological experiments[1].

Here, we demonstrate how automated patch clamp (APC) measurements of voltage-and ligand-gated ion channels, in combination with current-clamp measurements of action potentials, can be used to identify functionally comparable hiPSC-derived neurons for evaluating disease phenotypes.

The following hiPSC-derived neuronal cell lines were kindly provided by FUJIFILM Cellular Dynamics for the project:

- **iCell® GlutaNeurons**
- **iCell® Induced Excitatory Neurons – wildtype (WT)**
- **iCell® Induced Excitatory Neurons GRN R493X HZ KO (GRN)** - isogenic frontotemporal dementia disease model

The study includes:

- A Qube assay for functional characterization and disease evaluation of hiPSC-derived neurons yielding a whole-cell success rate of ~ 60 %
- Electrophysiological profiles of three hiPSC neuron cell lines, showing the percentage of neurons in which we could measure ion-channel currents (voltage- and ligand-gated) and action potentials
- A functional classification of hiPSC-derived neurons based on single-cell action potential firing pattern.
- An example of how this functional classification can be used for evaluation of disease phenotypes in a frontotemporal dementia disease model (GRN) showing:
  1. functional maturity is hampered in GRN neurons, as compared to isogenic control neurons (WT)
  2. a decreased voltage-gated Na^+ current density in GRN as compared to WT neurons that correlated with action-potential parameters

Results and discussion

Automated patch clamp assay for electrophysiological characterization of hiPSC-derived neurons

First, we developed an APC assay using hiPSC-derived cortical glutamatergic neurons (iCell GlutaNeurons). By optimizing the dissociation of the neuronal network (see methods for details) we obtained ~60 % whole-cell success rates on both Qube and QPatch.

Figure 1A displays a partial plate view of the Qube consumable, showing 96 out of 384 experiment sites. The experiment was running sequential measurement protocols (Figure 1B) to record voltage-gated Na^+ and K^+ channels (liquid addition 1); action potentials using current clamp (liquid addition 2) and ligand-gated (AMPA; NMDA or GABA) ion channels (liquid addition 3). Typically, these three protocols were repeated in the presence of chemical modulators, depending on the ion channel or disease phenotype being investigated. Figure 1C shows the success rate of each measurement upon application of filter criteria (listed in Table 2).

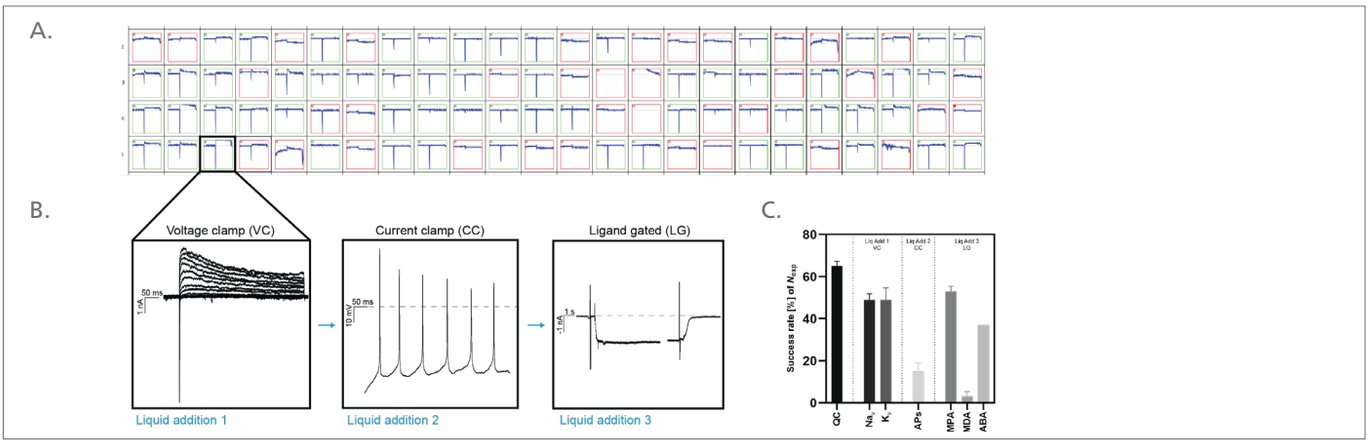

Fig. 1: Automated patch clamp assay for functional characterization of hiPSC-derived neurons. A) Partial plate view (displaying 96 out of 384 sites) of the experiment consumable. Each site harbors a single cell and has passed (green border) or failed (red border) membrane patch quality control (QC) filters. B) On each cell sequential protocols were run to perform voltage-clamp (liquid addition 1); current-clamp (liquid addition 2); and ligand-gated measurements. C) Measurement success rates in % of applied experiment sites (N_{exp}). The leftmost bar depicts the % of sites that pass QC filters, followed by the % of sites in which we recorded Na_V currents; K_V currents; action potentials; AMPA currents; NMDA currents; and GABA currents. Filter criteria are listed in Table 1.

Table 1: Applied filter criteria. Table detailing experiment protocol (left); measurement (middle) and filter criteria (right).

Experiment protocol	Measurement	Filter criteria
All	Quality control filters	Membrane resistance: R_{mem} > 200 MΩ Cell capacitance: C_{slow} > 2 pF
Liquid addition 1: voltage clamp	Na_V currents	Na_V peak current: $\|I_{Nav}\|$ > 100 pA
	K_V currents	K_V peak current: $\|I_{peak}\|$ > 200 pA K_V steady state current: $\|I_{ss}\|$ > 30 pA
Liquid addition 2: current clamp	Action potentials	Number of peaks: $N_{peak} \geq 2$ Action potential amplitude: APA > 30 mV Peak potential: V_p > -10 mV
Liquid addition 3: ligand-gated	AMPA; NMDA; GABA	Ligand-mediated current: $\|I_{Ligand}\|$- $\|I_{blocker}\|$> 15 pA

Electrophysiological characterization of a frontotemporal dementia disease model

Next, we used the assay for an electrophysiological characterization of a frontotemporal dementia (FTD) disease model. In about 20% of familial FTD, the disease is caused by mutations in the GRN gene causing lower levels of progranulin (PGRN). This protein and its derivatives have been implicated in cellular pathologies such as lysosomal dysfunction and neuroinflammation that eventually result in neuron degeneration[2,3]. Here, we compare iCell Induced Excitatory Neurons (WT), with an isogenic FTD disease model, iCell Induced Excitatory Neurons GRN R493X heterozygous knockout (GRN) (see methods).

For each of the three cell lines (glutamatergic neurons; WT excitatory neurons and GRN excitatory neurons) we quantified the percentage of neurons with a given electrophysiological property (ion channel current or action potentials). The resulting electrophysiological profiles were plotted in Figure 2. The excitatory neurons were recorded at two different time-points to investigate how their electrophysiological properties change over time.

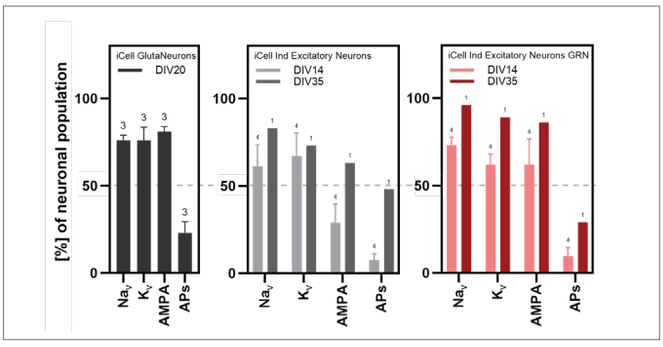

Fig. 2: Electrophysiological profile of three hiPSC-derived neuron cell lines (iCell GlutaNeurons, iCell Induced Excitatory Neurons and iCell Induced Excitatory Neurons GRN). The bar diagrams display the percentage of neuronal populations in which we can record a given electrophysiological phenotype, including ion channel currents and action potentials. For the excitatory neurons, the electrophysiological profile was recorded at two different maturation days *in vitro* (DIV) to evaluate how their electrophysiological properties change over time.

When comparing GRN and WT excitatory neurons they displayed differences in their electrophysiological profile and how they developed over time, especially the GRN neurons showed AMPA currents in a greater and action potentials in a smaller proportion of the cells.

Classification of neurons based on action potential firing patterns

hiPSC-derived neurons exhibit inherent intracelluar variability between cells, which can distort the pathophysiological evaluation of a disease model. To ensure accurate assessments, it is therefore important to compare neurons with equivalent electrophysiological maturity. Therefore, we performed a functional classification of the WT and GRN excitatory neurons, based on their action potential (AP) firing pattern (inspired by Bardy *et al.*, 2016). We executed a current step protocol (see methods) and

analyzed the APs at the current step that elicited the highest number of action potential peaks (N_p) that pass the filter criteria listed in Table 1. The neurons were then sorted into four functional types depending on their firing pattern (Figure 3A):

Type 1 (T1) neurons were not able to fire APs

- Type 2 (T2) neurons fired a single AP
- Type 3 (T3) neurons fired 2 APs
- Type 4 (T4) neurons fired more than 2 APs

As expected, for the WT excitatory neurons, the proportion of type 4 neurons increased as a function of maturation days *in vitro* (DIV) (figure 3B) and the trend was reproducible on two APC platforms (QPatch and Qube). We evaluated membrane parameters (membrane resistance, capacitance and resting membrane potential (RMP)) for the different neuron types (Figure 3C-E), and found a significant increase in capacitance, i.e. cell size, and a significant decrease in the resting membrane potential, as might be expected in more functionally mature neurons. As no significant changes in the parameters were observed as a function of DIV, all time points were grouped together.

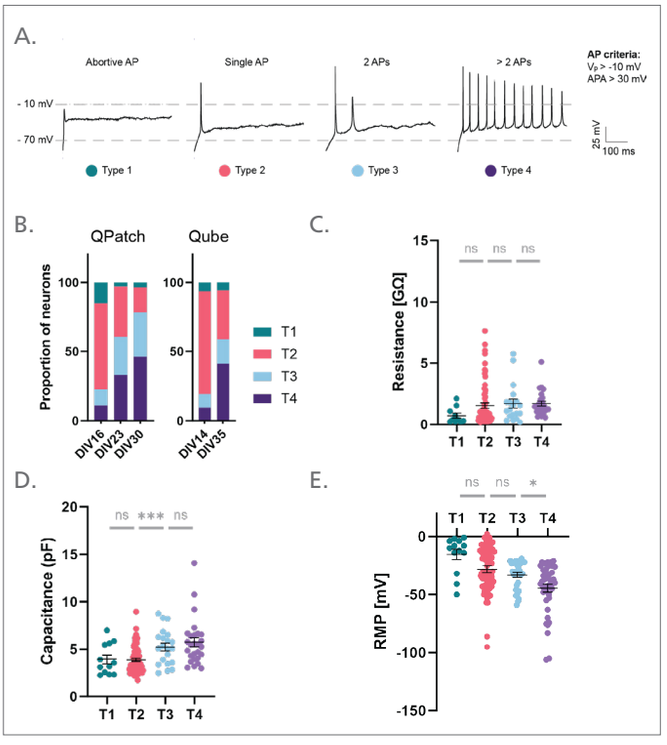

Fig. 3: Classification of WT excitatory neurons based on action potential firing pattern. A) Representative neuronal responses recorded at 0 pA holding current for 500 ms. We classified the neurons based on the number of APs fired (with V_p > -10 mV and APA > 30 mV) into four functional types. B) Bar diagram depicting the proportion of neurons in the four categories (T1, T2, T3 and T4) versus maturation days in vitro (DIV) quantified on two APC systems (QPatch and Qube). Plots of whole-cell resistance C); capacitance D); and resting membrane potential (RMP) E) versus neuron type (combining data from all time points). Each data point represents a single cell and the avg ± sem of the population is shown in black. Statistical comparisons are unpaired t-test with 95% confidence interval.

Evaluating the electrophysiological properties of the four functional neuron types (Figure 4), we observe increased Na_v current density (Figure 4B), a slightly decreased steady-state K_v current density (Figure 4D) and an increased proportion of neurons with AMPA currents (Figure 4E) in the more functionally mature neurons. As no significant changes were observed as a function of DIV, all time points were grouped together.

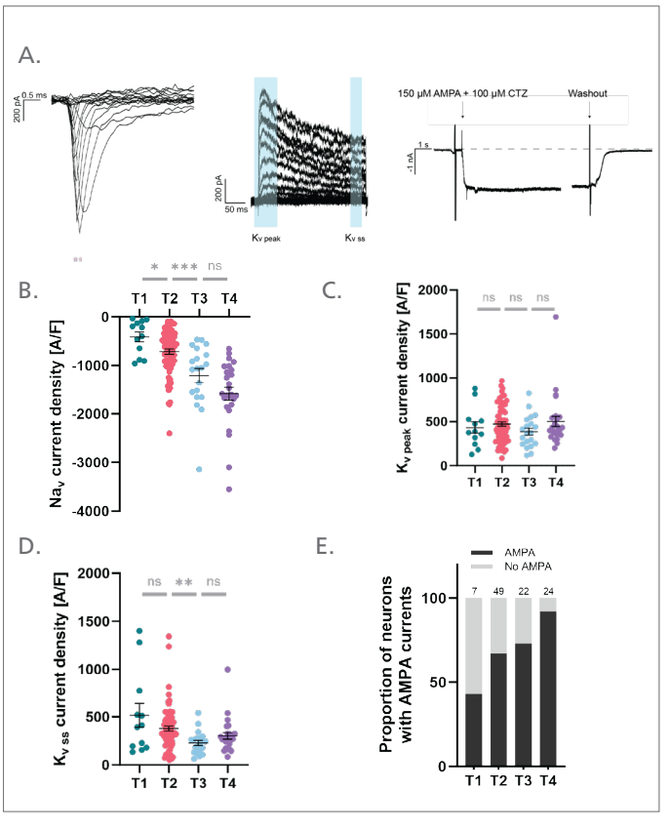

Fig. 4: Comparison of ion-channel currents in the four functional types of the WT excitatory neurons. A) Representative currents from the investigated ion channels. From left to right: voltage-gated Na^+ current; voltage-gated K^+ current; and AMPA Receptor current elicited by the application of 150 µM AMPA + 100 µM CTZ. The maximum Na_v B), K_v peak C), and $K_{v\,ss}$ D) current density [A/F] were plotted versus neuron type (combining data from all time points). Each data point represents a single cell and the avg ± sem of the population is shown in black. Statistical comparisons are unpaired t-test with 95% confidence interval. E) The proportion of neurons with AMPA-mediated currents versus neuron type.

GRN neurons contain a lower proportion of functionally mature neurons and show distinct differences in ion channel currents as compared to WT neurons

Finally, we classified the GRN neurons and plotted the proportion of neurons in each category as a function of maturation time together with WT neurons (Figure 5A). We found that the proportion of functionally mature (T4) neurons was lower in GRN than WT neurons and did not increase over maturation time. This finding could be reproduced across platforms (Qube and QPatch, Figure 5A) and agrees with MEA and live-cell imaging studies (Figure 9) which found a lower burst percentage and shorter neurite outgrowth in GRN compared to WT neuron networks. When comparing T4 neuron electrophysiology in WT and GRN excitatory neurons, we observe that GRN neurons were larger (higher capacitance, Figure 5B), had significantly higher AMPA current density, and significantly lower Na_V current density compared to WT.

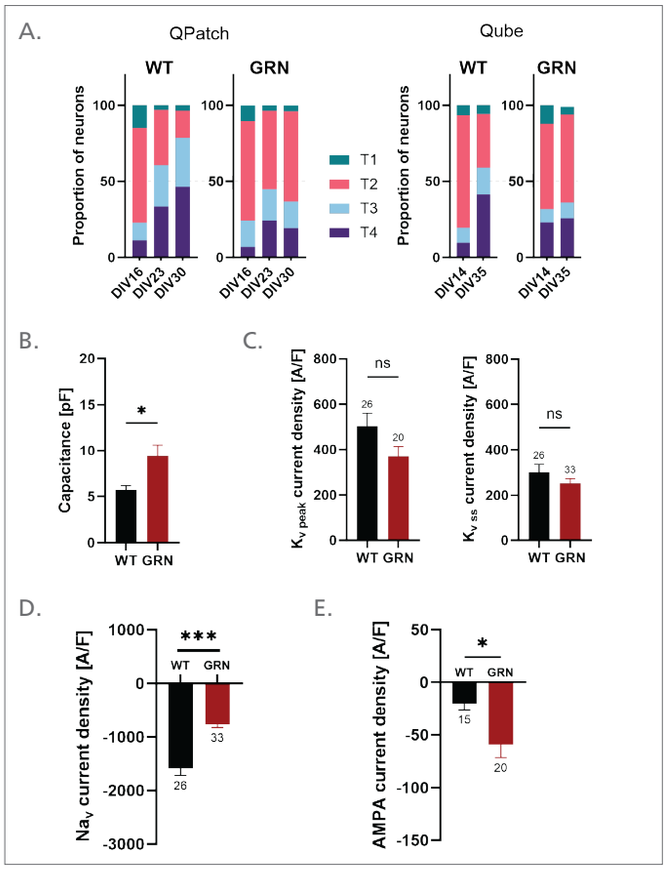

Fig. 5: GRN neurons display a lower proportion of functionally mature neurons and distinct electrophysiological properties as compared to WT. A) Bar diagram depicting the proportion of WT and GRN neurons, respectively, in the four categories (T1, T2, T3 and T4) versus maturation days *in vitro* (DIV) quantified on two APC systems (Qpatch and Qube). We extracted following electrophysiological measurements for WT (black) and GRN (red) T4 neurons: B) C_{slow}; C) $K_{V\ peak}$ and $K_{V\ ss}$ current density; D) Na_V current density; and E) AMPA current density. Bars represent avg ± sem of the neuron population. Statistical comparisons are unpaired t-test with 95% confidence interval.

The lower Na_V current density in GRN compared to WT T4 neurons (Figure 5D), translates into differences in AP parameters (see Table 2 and Figure 6). We quantified on average a lower peak potential (V_p), lower action potential amplitude (APA) and slower depolarization rate (MDR) in GRN compared to WT T4 neurons. This finding aligns with MEA studies showing a longer time to peak in GRN compared to WT neuronal networks (Figure 9B).

Table 2: Extracted AP parameters. We executed a current-step protocol (see methods) and analyzed the APs at the current step (I_{hold}) that elicited the highest number of AP peaks (N_p). The table lists from the left; the extracted AP parameter; avg ± sem extracted for WT neurons; avg ± sem extracted for GRN neurons; P-value; significance of difference. Statistical comparisons are unpaired t-test with 95% confidence interval.

Action potential parameter	WT N_{cells}=41	GRN N_{cells}=14	P-value	Significance
Threshold potential - V_t [mV]	-40.3±0.7	-38.3±0.8	0.0574	ns
Peak potential - Vp [mV]	17±2	9±2	0.0006	***
Hyperpolarization potential - V_h [mV]	-52.5±0.8	-52.6±0.9	0.9121	ns
Action potential amplitude - APA [mV]	69±2	61±2	0.0069	***
Action potential duration at 90% - ADP90 [ms]	5.8±0.5	5.5±0.4	0.6678	ns
Action potential duration at 50% - ADP50 [ms]	2.6±0.2	2.7±0.2	0.8102	ns
Maximum depolarization rate - MDR [V/s]	94±5	67±5	0.0002	***
Maximum repolarization rate - MRR [V/s]	-27±2	-23±2	0.0862	ns
Peak frequency - Freq [s^{-1}]	21±2	18±1	0.1920	ns
Rheobase current - I_{Rheo} [pA]	-13±2	-19±3	0.1220	ns
Maximum no. of peaks - $N_{p\ max}$	7.9±0.6	7.3±0.6	0.4674	ns

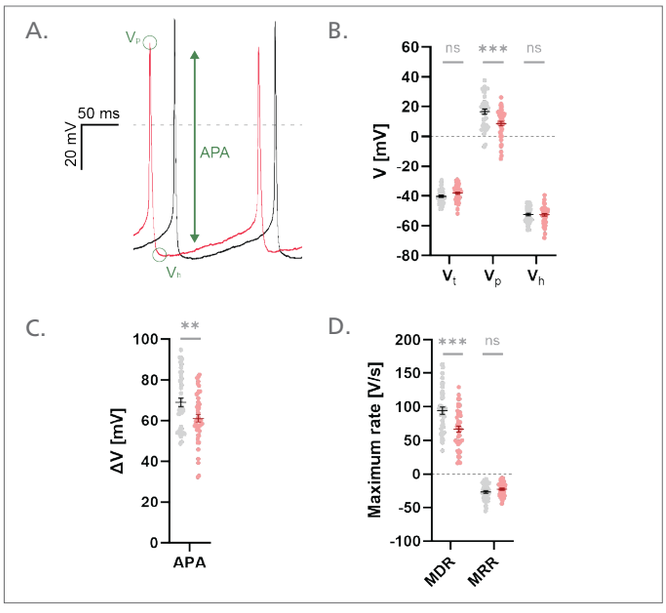

Fig. 6: Plot of selected AP parameters in WT and GRN excitatory neurons. A) Representative APs recorded in WT (black) and GRN (red) excitatory neurons. B) Plot of threshold potential (V_t), peak potential (V_p) and hyperpolarization potential (V_h) for WT (grey) and GRN (red) excitatory neurons. C) Plot of action potential amplitude (APA) for WT (grey) and GRN (red) excitatory neurons. D) Plot of maximum depolarization rate (MDR) and maximum repolarization rate (MRR) for wild-type (WT, grey) and GRN (red) excitatory neurons. Each data point represents a single cell, and the average ± sem of the population is shown in black or dark red for WT and GRN, respectively. Statistical comparisons are unpaired t-test with a 95% confidence interval.

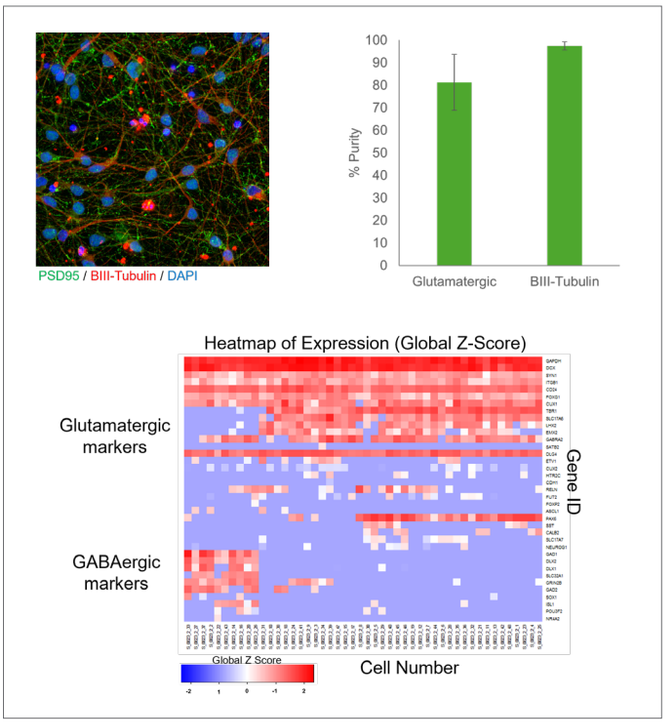

Fig. 7: Characterization iCell GlutaNeurons. A) Representative immunostaining of iCell GlutaNeurons for BIII-Tubulin (red), PSD95 (green), and DAPI (blue) on Day 7 post-thaw highlights robust and healthy neural cultures. Images provided by Cell Signaling Technology. B) iCell GlutaNeurons are highly pure with ≥ 90% positive for the neural marker BIII-tubulin (flow cytometry) and ~75% glutamatergic (single cell gene expression). C) Single-cell gene expression analysis confirms the majority of the population is cortical glutamatergic neurons.

Methods

Development and characterization of hiPSC-derived excitatory neurons

iCell GlutaNeurons (Cat # R1061) iCell Induced Excitatory Neurons (Cat # R1245) and iCell Induced Excitatory Neurons GRN R493 HZ KO (Cat # R1247) were kindly provided by FUJIFILM Cellular Dynamics. Cells were cultured according to the manufacturer's user guide.

iCell GlutaNeurons are an enriched population of cortical-specified human iPSC-derived glutamatergic neurons which utilize a directed differentiation protocol for manufacturing (Figure 7). Complementary to iCell GlutaNeurons are iCell Induced Excitatory Neurons, which are forward programmed using neurogenin-2 NGN2 overexpression in human iPSCs. This method produces a highly pure glutamatergic neuron population that is not regionally specified.

Characterization of apparently healthy normal (AHN) and the frontotemporal dementia excitatory neurons (genetically engineered Granulin R493X heterozygous knockout (GRN)) showed robust neuronal populations and similar gene expression profiles (Figure 8). MEA measurements recorded at DIV 28 showed different neuronal activity patterns in GRN vs AHN, with GRN consistently having longer time to burst peak compared to AHN (Figure 9A and B). In addition, neurite length was quantified daily from DIV 0 to DIV 14 using the IncuCyte® Live-Cell Analysis System, and GRN neurons were found to have reduced neurite length compared to WT neurons (Figure 9C).

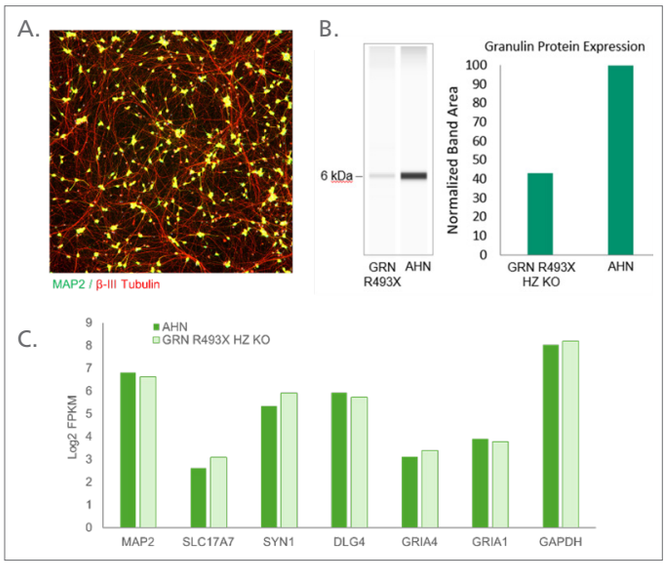

Fig. 8: Characterization of AHN and GRN R493X iCell Induced Excitatory Neurons. A) Representative immunostaining of iCell Induced Excitatory Neurons (AHN) for MAP2 (green) and β-III Tubulin (red) on Day 7 post-thaw highlights robust and healthy neural cultures. B) iCell Induced Excitatory Neurons GRN R493X were analyzed by Western blot for granulin protein expression, and the cleaved GRN fragments of ~6 kDa were much more lightly expressed in the HZ GRN neurons as compared to AHN control. C) Comparison of post-thaw qPCR gene expression analysis of AHN and GRN R493X HZ KO-induced neurons revealed a consistent and primarily excitatory glutamatergic neuronal population. Cells showed high expression of vesicular glutamate transporters (vGlut2), and AMPA receptor subunits (GRIA1, 4), synaptic genes (SYN1 and DLG4/PSD95) and neuronal markers (MAP2)[4].

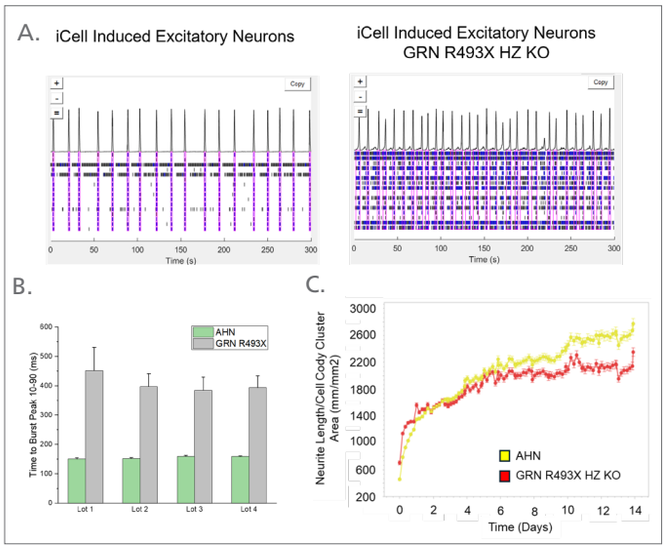

Fig. 9: MEA and Neurite Outgrowth of AHN and GRN R493X iCell Induced Excitatory Neurons A) iCell Induced Excitatory Neurons (AHN and GRN R493X HZ KO) neural activity recorded at 21 days using Axion Maestro shows different neural activity patterns. B) Time to Burst Peak is a consistent parameter showing neural network differences, with GRN neurons having longer time burst peak compared to AHN. C) iCell Induced Excitatory Neurons (AHN and GRN R493X HZ KO) were cultured and neurite length measured through a 14-day culture. Data show reduced neurite length in the GRN neurons.

Sophion Bioscience A/S
info@sophion.com
sophion.com

Preparation of the cell suspension

iCell GlutaNeurons were harvested at days *in vitro* (DIV) 20 and used for Qube experiments. iCell Induced Excitatory Neurons were harvested at DIV 16, 23, and 30 (for QPatch) and DIV 14 and 35 (for Qube). On the day of experiment the cells were dissociated according to Sophion's in-house procedures, specifically optimized for these neurons (for more information contact us at info@sophion.com). Dissociated neurons, in a pure, homogenous suspension with a cell density of (1-2) mio/mL, were added to the APC instrument of choice.

Voltage protocols

The three voltage protocols utilized were:

1. Voltage step protocol for recordings of Na_v and K_v currents: A 200 ms pre-step at -120 mV followed by 300 ms voltage steps from -90 mV to + 60 mV (ΔV = 10 mV)
2. Current step protocol for recordings of action potentials: A 20 ms pre-step at -70 mV followed by 500 ms current steps from -50 pA to + 100 pA (ΔI = 10 pA)
3. Ligand-gated currents were recorded at constant V = -70 mV (for NMDA and AMPA) or V = 0 mV (for GABA).

Compounds and solutions

Na_v channels were blocked using 1 µM TTX. K_v channels were partially blocked using 4 mM 4-AP and 30 mM TEA. AMPARs were activated by addition of 150 µM AMPA in the presence of 100 µM CTZ (PAM), followed by washout by saline or block by 20 µM NBQX. NMDARs were activated by 50 µM NMDA in the presence of 50 µM glycine and 1 µM GNE9278 (PAM), followed by washout with saline or block by 100 µM D-AP5. GABARs were activated by the addition of 100 µM GABA in the presence of 100 nM diazepam (PAM), followed by washout with saline or block by 300 µM picrotoxin.

References

1. Bardy, C. et al. Predicting the functional states of human iPSC-derived neurons with single-cell RNA-seq and electrophysiology. *Mol Psychiatry* **21**, 1573–1588 (2016).
2. Rhinn, H., Tatton, N., McCaughey, S., Kurnellas, M. & Rosenthal, A. Progranulin as a therapeutic target in neurodegenerative diseases. *Trends in Pharmacological Sciences* vol. 43 641–652 Preprint at https://doi.org/10.1016/j.tips.2021.11.015 (2022).
3. Amin, S., Carling, G. & Gan, L. New insights and therapeutic opportunities for progranulin-deficient frontotemporal dementia. *Current Opinion in Neurobiology* vol. 72 131–139 Preprint at https://doi.org/10.1016/j.conb.2021.10.001 (2022).
4. Lin, H. C. et al. NGN2 induces diverse neuron types from human pluripotency. *Stem Cell Reports* **16**, 2118–2127 (2021).

Author:

Kadla Rosholm, Senior Research Scientist

iCell GlutaNeurons (Cat # R1061) iCell Induced Excitatory Neurons (Cat # R1245) and iCell Induced Excitatory Neurons GRN R493 HZ KO (Cat # R1247) were kindly provided by:

FUJIFILM
Value from Innovation